

1 **Trend of atmospheric mercury concentrations at Cape Point for 1995**
2 **– 2004 and since 2007**

3

4 Lynwill G. Martin¹, Casper Labuschagne¹, Ernst-Günther Brunke¹, Andreas Weigelt^{2*},
5 Ralf Ebinghaus², Franz Slemr³

6

7 ¹South African Weather Service c/o CSIR, P.O.Box 320, Stellenbosch 7599, South
8 Africa

9 ²Helmholtz-Zentrum Geesthacht (HZG), Institute of Coastal Research, Max-Planck-
10 Strasse 1, D-21502 Geesthacht, Germany,

11 ³Max-Planck-Institute for Chemistry, Hahn-Meitner-Weg 1, D-55128 Mainz, Germany
12

13 *now at: Federal Maritime and Hydrographic Agency (BSH), D-22589 Hamburg,
14 Germany

15

16

17 Lynwill Martin: lynwill.martin@weathersa.co.za

18 Casper Labuschagne: casper.labuschagne@weathersa.co.za

19 Ernst-Günther Brunke: egbrunke@gmail.com

20 Andreas Weigelt: andreas.weigelt@bsh.de

21 Ralf Ebinghaus: ralf.ebinghaus@hzg.de

22 Franz Slemr: franz.slemr@mpic.de

23

24

25 **Abstract**

26

27 Long-term measurements of gaseous elemental mercury (GEM) concentrations at Cape
28 Point, South Africa, reveal a downward trend between September 1995 and December
29 2005 and an upward one since March 2007 until June 2015 implying a change in trend
30 sign between 2004 and 2007. The trend change is qualitatively consistent with the trend
31 changes in GEM concentrations observed at Mace Head, Ireland, and in mercury wet
32 deposition over North America suggesting a change in worldwide mercury emissions.

33

34 Seasonally resolved trends suggest a modulation of the overall trend by regional
35 processes. The trends in absolute terms (downward in 1995 – 2004 and upward in 2007
36 – 2015) are the highest in austral spring (SON) coinciding with the peak in emissions
37 from biomass burning in South America and southern Africa. The influence of trends
38 in biomass burning is further supported by a biennial variation in GEM concentration
39 found here and an ENSO signature in GEM concentrations reported recently.

40

41

42 **Introduction**

43

44 Mercury and especially methyl mercury which bio-accumulates in the aquatic
45 nutritional chain are harmful to humans and animals (e.g. Mergler et al., 2007;
46 Scheuhammer et al., 2007; Selin, 2009; and references therein). Mercury, released into
47 the environment by natural processes and by anthropogenic activities, cycles between
48 the atmosphere, water, and land reservoirs (Selin et al., 2008). In the atmosphere,
49 mercury occurs mostly as gaseous elemental mercury (GEM) which with an
50 atmospheric lifetime of 0.5 – 1 yr can be transported over large distances (Lindberg et
51 al., 2007). Mercury is thus a pollutant of global importance and as such on the priority
52 list of several international agreements and conventions dealing with environmental
53 protection and human health, including the United Nations Environment Program
54 (UNEP) Minamata convention on mercury (www.mercuryconvention.org).

55

56 Because of fast mixing processes in the atmosphere, monitoring of tropospheric
57 mercury concentrations and of its deposition will thus be the most straightforward way
58 to verify the decrease of mercury emissions expected from the implementation of the
59 Minamata convention. Regular monitoring of atmospheric mercury started in the mid-
60 1990s with the establishment of mercury monitoring networks in North America
61 (Temme et al., 2007; Prestbo and Gay, 2009; Gay et al., 2013). Until 2010 only a few
62 long-term mercury observations have been reported from other regions of the northern
63 hemisphere and hardly any from the southern hemisphere (Sprovieri et al., 2010). The
64 Global Mercury Observation System (GMOS, www.gmos.eu) was established in 2010
65 to extend the mercury monitoring network, especially in the southern hemisphere
66 (Sprovieri et al., 2016).

67

68 Decreasing atmospheric mercury concentrations and wet mercury deposition have been
69 reported for most sites in the northern hemisphere (Temme et al., 2007; Prestbo and
70 Gay, 2009; Ebinghaus et al., 2011; Gay et al., 2013). At Cape Point, the only site in the
71 southern hemisphere with a long-term record exceeding a decade, decreasing mercury
72 concentrations were also observed between 1996 and 2004 (Slemr et al., 2008). The
73 worldwide decreasing trend has been at odds with increasing mercury emissions in most
74 inventories (Muntean et al., 2014, and references therein). Soerensen et al. (2012)

75 thought that decreasing mercury concentrations in sea water of the North Atlantic were
76 responsible for the decrease, at least in the northern hemisphere. The most recent
77 inventories, however, attribute the decrease of atmospheric mercury concentrations to
78 a decrease in mercury emissions since 1990 (Zhang et al., 2016). The decrease in
79 mercury emissions was attributed to the decrease of emissions from commercial
80 products, changing speciation of emission from coal-fired power plants, and to the
81 improved estimate of mercury emissions from artisanal mining. According to Zhang et
82 al. (2016) the worldwide anthropogenic emissions decreased from 2890 Mg yr⁻¹ in 1990
83 to 2160 Mg yr⁻¹ in 2000 and increased slightly to 2280 Mg yr⁻¹ in 2010.

84
85 In the first approximation, the observed trends in atmospheric mercury should follow
86 these changes. There is indeed some recent evidence that the downward trend in the
87 northern hemisphere is slowing or even turning upwards (Weigelt et al., 2015; Weiss-
88 Penzias et al., 2016). Here we report and analyse the trends of atmospheric mercury
89 concentrations at the GAW station Cape Point between 1995 and 2004 and since March
90 2007 until June 2015.

91 **Experimental**

92
93
94 The Cape Point site (CPT, 34° 21'S, 18° 29'E) is operated as one of the Global
95 Atmospheric Watch (GAW) baseline monitoring observatories of the World
96 Meteorological Organization (WMO). The station is located on the southern tip of the
97 Cape Peninsula within the Cape Point National Park on top of a peak 230 m above sea
98 level and about 60 km south from Cape Town. The station has been in operation since
99 the end of the 1970s and its current continuous measurement portfolio includes Hg, CO,
100 O₃, CH₄, N₂O, ²²²Rn, CO₂, several halocarbons, particles, and meteorological
101 parameters. The station receives clean marine air masses for most of the time.
102 Occasional events with continental and polluted air can easily be filtered out using a
103 combination of CO and ²²²Rn measurements (Brunke et al., 2004). Based on the ²²²Rn
104 ≤ 250 mBq m⁻³ criterion about 35% of the data are classified annually as baseline.

105
106 Gaseous elemental mercury (GEM) was measured by a manual amalgamation
107 technique (Slemr et al., 2008) between September 1995 and December 2004 and by the
108 automated Tekran 2537B instrument (Tekran Inc., Toronto, Canada) since March 2007.
109 Typically, ~ 13 measurements per month were made using the manual technique, each
110 covering 3 h sampling time. The manual technique was compared with the Tekran
111 technique in an international intercomparison (Ebinghaus et al., 1999) and provided
112 comparable results.

113
114 Since March 2007 GEM was measured using an automated dual channel, single
115 amalgamation, cold vapor atomic fluorescence analyzer (Tekran-Analyzer Model 2537
116 A or B, Tekran Inc., Toronto, Canada). The instrument utilized two gold cartridges.
117 While one is adsorbing mercury during a sampling period, the other is being thermally
118 desorbed using argon as a carrier gas. Mercury is detected using cold vapor atomic
119 fluorescence spectroscopy (CVAFS). The functions of the cartridges are then
120 interchanged, allowing continuous sampling of the incoming air stream. Operation and
121 calibration of the instruments follow established and standardized procedures of the
122 GMOS (Global Mercury Observation System, www.gmos.eu) project. The instrument
123 was run with 15 min sampling frequency while 30 min averages were used for the data

124 analysis. All mercury concentrations reported here are given in ng m^{-3} at 273.14 K and
125 1013 hPa.

126

127 The Mann-Kendal test for trend detection and an estimate of Sen's slope were made
128 using the program by Salmi et al. (2002).

129

130 **Results and discussion**

131

132 The upper panel of Figure 1 shows monthly average GEM concentrations calculated
133 from all data since March 2007 until June 2015 and in the lower panel monthly average
134 GEM concentrations were calculated from baseline data, i.e. GEM concentrations
135 measured at ^{222}Rn concentration $\leq 250 \text{ mBq m}^{-3}$. The slope of the least square fit of all
136 data ($0.0222 \pm 0.0032 \text{ ng m}^{-3} \text{ yr}^{-1}$) is not significantly different from the slope calculated
137 from the baseline data only ($0.0219 \pm 0.0032 \text{ ng m}^{-3} \text{ yr}^{-1}$). Sen's slope and trend
138 significance for all ($0.0210 \text{ ng m}^{-3} \text{ yr}^{-1}$) and baseline ($0.0208 \text{ ng m}^{-3} \text{ yr}^{-1}$) data are listed
139 in Table 1. Sen's slopes tend to be somewhat lower than the slopes from the least square
140 fits but they are in agreement within their 95% uncertainty range. All trends are highly
141 significant, i.e. at level $\geq 99.9\%$. The results are essentially the same whether monthly
142 median or monthly average concentrations are used. This shows that the trend is robust
143 and not influenced by occasional pollution or depletion events (Brunke et al., 2010,
144 2012).

145

146 For comparison we also calculated the trends for the manually measured GEM
147 concentrations during the period September 1995 – December 2004 periods. These data
148 have an annual coverage of only about 300 hours per year, i.e. about 3% in contrast to
149 the Tekran measurements since 2007 where the coverage was nearly 100%. Baseline
150 data were not filtered out from this data set because a) on average only 13 measurements
151 were available per month and b) ^{222}Rn was measured only since March 1999 and cannot
152 thus be used as criterion for the whole period. In Table 2 we list the trends calculated
153 from the least square fit of the monthly medians. Monthly averages provide
154 qualitatively the same trends with lower significance, because of their larger sensitivity
155 to extreme GEM concentrations. The trend of all monthly medians of -0.0176 ± 0.0027
156 $\text{ng m}^{-3} \text{ year}^{-1}$ is somewhat higher than $-0.015 \pm 0.003 \text{ ng m}^{-3} \text{ year}^{-1}$ (Slemr et al., 2008)
157 calculated from the 1996 and 1999 – 2004 annual averages but within the uncertainty
158 of both calculations.

159

160 The upward trend after March 2007 and the downward trend between 1995 and 2004
161 were measured by different techniques: the former one with a Tekran instrument and
162 the latter one using the manual technique. For reasons outside of our control we could
163 not operate both techniques side by side for a reasonable length of time. Although the
164 measurements by both techniques agreed well during an international field
165 intercomparison (Ebinghaus et al., 1999), we do not claim here that they are comparable
166 without an extended intercomparison of both techniques at Cape Point. Assuming
167 internal consistency of each of the data sets, it is however obvious that the decreasing
168 trend between 1995 and 2004 turned to an increasing one since 2007 implying that the
169 turning point was located between 2004 and 2007.

170

171 The trend reversal at Cape Point is the most pronounced but not the only evidence that
172 the hemispheric trends in mercury concentrations are changing. An analysis of 1996 –
173 2013 data from Mace Head, classified according to the geographical origin of the air

174 masses, showed a) that the downward trend of mercury concentration in air masses
175 originating from over the Atlantic Ocean south of 28°N is substantially lower than for
176 all other classes originating north of 28°N and b) that all downward trends for air masses
177 originating from north of 28°N are decelerating (Weigelt et al., 2015). The apparent
178 inconsistency that no decelerating trend for air masses from south of 28°N was found
179 can be explained by the fact that the changes of a smaller trend are likely to be more
180 difficult to detect. Weiss-Penzias et al. (2016) recently reported that the wet mercury
181 deposition was decreasing at 53% of the sites in the U.S. and Canada and was increasing
182 at none of the sites over the period 1997 – 2013. Over the period 2008-2013, however,
183 the mercury wet deposition was decreasing only at 6% of the sites but was increasing
184 at 30% of the sites. Thus the sign change of the trend at Cape Point somewhere between
185 2004 and 2007 is just one more indication that trends in atmospheric mercury
186 concentrations are changing world-wide.

187

188 Trends in mercury concentrations and mercury wet deposition are most likely related
189 to changes in worldwide emission (Pacyna et al., 2016). Most anthropogenic emission
190 inventories show nearly constant or increasing anthropogenic emissions between 1990
191 and 2010 (Wilson et al., 2010; Streets et al., 2011; Muntean et al., 2014) which is
192 inconsistent with the worldwide decreasing trend in atmospheric mercury
193 concentrations and mercury wet deposition over this period. This inconsistency has
194 been explained by decreasing emissions from North Atlantic Ocean due to reduced
195 mercury concentrations in subsurface ocean water (Soerensen et al., 2012) and more
196 recently by a substantial reduction of mercury emissions from coal fired power plants
197 and from commercial products between 1990 and 2000 (Zhang et al., 2016). The most
198 recent inventory by Zhang et al. (2016) estimated that the worldwide anthropogenic
199 emissions decreased from 2890 Mg yr⁻¹ in 1990 to 2160 Mg yr⁻¹ in 2000 and increased
200 slightly to 2280 Mg yr⁻¹ in 2010. To the best of our knowledge no more recent emission
201 estimates have been published so far (the emission estimates are always delayed by
202 several years needed for the collection of the underlying statistical data). Since the
203 potential to reduce emissions from the commercial products and from coal fired power
204 plants was largely exhausted between 1990 and 2000 a further increase of worldwide
205 mercury emissions between 2010 and 2015, mostly from increasing coal burning and
206 artisanal small scale gold mining can be expected.

207 Seasonally resolved trends may provide some information about the processes
208 influencing the trends at Cape Point. The trends were calculated for different seasons
209 (austral fall - March, April, May; winter – June, July, August; spring – September,
210 October, November; and summer – December, January, February) for the period since
211 March 2007 until June 2015 from all and baseline data. These are listed in Table 1.
212 Although the 95% uncertainty ranges of seasonal Sen's slopes overlap, the least square
213 fit slopes for different seasons are statistically different at > 99% significance level.
214 Irrespective of whether monthly averages or medians or least square fit or Sen's slope
215 are used, a consistent picture emerges with upward trends where the slopes decrease in
216 the following order: austral spring (SON) > summer (DJF) > winter (JJA) > fall
217 (MAM). Seasonal trends for the 1995 – 2004 period shown in Table 2 are all downward
218 and their slopes are decreasing in the following order: austral fall > summer > winter >
219 spring (note the negative sign of the slopes). The difference between fall and summer
220 as well as between winter and spring is not significant. In absolute terms the slope
221 during austral autumn (MAM) is the smallest and for spring (SON) is the highest for
222 both the 1995 – 2004 and 2007 – 2015 data sets.

223

224 The difference in seasonal GEM trends could originate from the seasonal trends of
225 GEM emissions. Hg emissions from coal fired power plants, the largest anthropogenic
226 Hg source, tend to be nearly constant over the year (Rotty, 1997). On the contrary,
227 biomass burning is a highly seasonal phenomenon with maximum emissions during
228 August - September both in southern America and southern Africa (Duncan et al., 2003;
229 van der Werff et al., 2006). Taking into account a delay by ~ 3 months due to intra-
230 hemispherical air mixing time, October - November coincide with the maximum
231 absolute seasonal trends: an upward one for 2007 – 2015 and a downward one for the
232 1995 – 2004 periods. Biomass burning emission inventories suggest a small decrease
233 in CO emissions from Africa and more pronounced one from South America between
234 1997 and 2004, but differences between different inventories render it very uncertain
235 (Granier et al., 2011). As the emission estimates by Granier et al. (2011) end in 2010,
236 no trend in emissions from biomass burning in 2007 – 2015 period can be given.
237 Nonetheless, the ambient Cape Point CO data has shown a measurable decrease during
238 2003 till 2014 (Tohir et al., 2015). We tried to calculate seasonal trends of baseline CO
239 mixing ratios for 1995 – 2004 and 2007 – June 2015 periods but none of the trends was
240 significant. The 1995 – 2004 and 2007 – June 2015 periods are probably too short to
241 reveal trends in CO data obscured by strong seasonal and interannual variations.
242 Nevertheless, the ENSO signature both in Hg and CO data from Cape Point, Mace
243 Head, and CARIBIC was found to be consistent, within large uncertainty margins, with
244 emissions from biomass burning (Slemr et al., 2016). In summary, seasonal variations
245 of emissions from biomass burning in southern Africa and America as well as ENSO
246 signature are consistent with a hypothesis of emissions from biomass burning as a major
247 driving force behind the different seasonal trends as seen in the Cape Point data.

248

249 Seasonal variation of mercury concentrations was also investigated. For this we
250 detrended the monthly averages using their least square fits. The detrended monthly
251 averages were then averaged according to months. Figure 2a shows the seasonal
252 variation of relative monthly averages with their respective standard error. No
253 systematical seasonal variation is apparent in this plot. We noted, however, a two-year
254 periodicity in the monthly averages. Figure 2b shows the monthly averages of the
255 detrended monthly values for a 2 year period. Despite the somewhat higher standard
256 errors of the monthly averages (number of averaged months for biennial variation being
257 only half of those for the seasonal variation), the monthly averages vary between 0.95
258 and 1.05 as do the monthly averages for the seasonal variation (Figure 1a). Taken
259 collectively, however, the relative GEM concentrations during the second year are
260 significantly (>99.9%) higher than those in the first year. This is a clear sign of a
261 biennial variation of GEM concentrations at Cape Point.

262

263 Tropospheric biennial oscillations (TBO) in tropospheric temperature, pressure, wind
264 field, monsoon, etc. has been previously reported in the literature (e.g. Meehl, 1997,
265 Meehl and Arblaster, 2001, 2002, Zheng and Liang, 2005). Meehl and Arblaster (2001)
266 also report that TBO with roughly a 2 – 3 years period encompasses most ENSO years
267 with their well-known biennial tendency. Slemr et al. (2016) analysed mercury data
268 from Cape Point in South Africa, Mace Head in Ireland, and from CARIBIC
269 measurements in the upper troposphere and found an ENSO signature in all these data
270 sets. Thus the finding of biennial variation of GEM concentrations at Cape Point is
271 consistent with the ENSO influence.

272

273 **Conclusions**

274

275 We report here an upward trend for mercury concentrations at Cape Point for the period
276 2007 – 2015. As mercury concentrations at Cape Point decreased over the period 1995
277 – 2004 we conclude that the trend must have changed sign between 2004 and 2007.
278 Such a change is qualitatively consistent with the trend changes observed in
279 atmospheric mercury concentrations at Mace Head in the Northern Hemisphere
280 (Weigelt et al., 2015) and in mercury wet deposition at sites in North America (Weiss-
281 Penzias et al., 2016). Combining all this evidence it seems that the worldwide mercury
282 emissions are now increasing, after a decade or two of decreasing emissions. This
283 finding is consistent with the temporal development of mercury emissions in the most
284 recent mercury inventory (Zhang et al., 2016).

285

286 For both periods, 1995 – 2004 and 2007 – 2015, seasonally resolved trends were
287 different in different seasons. We believe that the observed trends of GEM
288 concentrations at Cape Point result from the trend of worldwide mercury emissions and
289 are additionally modulated by regional influences. During 1995 – 2004 the highest
290 downward trend was observed in austral spring (SON) and winter (JJA). For the 2007
291 – 2015 period the highest upward trend was found in austral spring. Hg emissions from
292 biomass burning in South America and southern Africa both peak in August and
293 September (Duncan et al., 2003, van der Werff et al., 2006). Although the trend of these
294 emissions is uncertain because of differences between different emission inventories
295 (Granier et al., 2013), it can produce different trends in different seasons. Biennial
296 variation of the GEM concentrations at Cape Point, reported here, suggest that
297 climatological changes of transport patterns can also play a role in seasonally different
298 trends. The detection of the ENSO signature in GEM concentrations at Cape Point
299 (Slemr et al., 2016) is consistent with the influence of both emissions from biomass
300 burning and changing regional transport patterns.

301

302

303 **Acknowledgment**

304

305 The GEM measurements made at Cape Point have been supported by the South
306 African Weather Service and have also received financial support from the Global
307 Mercury Observing System (GMOS), a European Community funded FP7 project
308 (ENV.2010.4.1.3-2). We are grateful to Danie van der Spuy for the general
309 maintenance of the Tekran analyser at Cape Point.

310

311

312 **References**

313

314 Brunke, E.-G., Labuschagne, C., Parker, B., Scheel, H.E., Whittlestone, S.: Baseline air
315 mass selection at Cape Point, South Africa: Application of ²²²Rn and other filter criteria
316 to CO₂, Atmos. Environ. 38, 5693-5702, 2004.

317

318 Brunke, E.-G., Kabuschagne, C., Ebinghaus, R., Kock, H.H., and Slemr, F.: Gaseous
319 elemental mercury depletion events observed at Cape Point during 2007 – 2008, Atmos.
320 Chem. Phys., 10, 1121-1131, 2010.

321

- 322 Brunke, E.-G., Ebinghaus, R., Kock, H.H., Labuschagne, C., Slemr, F.: Emissions of
323 mercury in southern Africa derived from long-term observations at Cape Point, South
324 Africa, *Atmos. Chem. Phys.* 12, 7465-7474, 2012.
- 325
326 Duncan, B.N., Martin, R.V., Staudt, A.C., Yevich, R., and Logan, J.A.: Interannual and
327 seasonal variability of biomass burning emissions constrained by satellite observations,
328 *J. Geophys. Res.*, 108; D2, 4100, doi:10.1029/2002JD002378, 2003.
- 329
330 Ebinghaus, R., Jennings, S.G., Schroeder, W.H., Berg, T., Donaghy, T., Guentzel, J.,
331 Kenny, C., Kock, H.H., Kvietkus, K., Landing, W., Mühleck, T., Munthe, J., Prestbo,
332 E.M., Schneeberger, D., Slemr, F., Sommar, J., Urba, A., Wallschläger, D., Xiao, Z.:
333 International field intercomparison measurements of atmospheric mercury species,
334 *Atmos. Environ.* 33, 3063-3073, 1999.
- 335
336 Ebinghaus, R., Jennings, S.G., Kock, H.H., Derwent, R.G., Manning, A.J., and Spain,
337 T.G.: Decreasing trend in total gaseous mercury observations in baseline air at Mace
338 Head, Ireland, from 1996 to 2009, *Atmos. Environ.* 45, 3475-3480, 2011.
- 339
340 Gay, D.A., Schmeltz, D., Prestbo, E., Olson, M., Sharac, T., and Tordon, R.: The
341 Atmospheric Mercury Network: measurement and initial examination of an ongoing
342 atmospheric mercury record across North America, *Atmos. Chem. Phys.*, 13, 11339-
343 11349, 2013.
- 344
345 Granier, C., Bessagnet, B., Bond, T., D'Angiola, A., Denier van der Gon, H., Frost,
346 G.J., Heil, A., Kaiser, J.W., Kinne, S., Klimont, Z., Kloster, S., Lamarque, J.-F.,
347 Lioussé, C., Masui, T., Meleux, F., Mieville, A., Ohara, T., Raut, J.-C., Riahi, K.,
348 Schultz, M.G., Smith, S.J., Thompson, A., van Aardenne, J., van der Werff, G.R., and
349 van Vuuren, D.P.: Evolution of anthropogenic and biomass burning emissions of
350 pollutants at global and regional scales during the 1980 – 2010 period, *Clim. Change*,
351 109, 163-190, 2011.
- 352
353 Lindberg, S., Bullock, R., Ebinghaus, R., Engstrom, D., Feng, X., Fitzgerald, W.,
354 Pirrone, N., Prestbo, E., and Seigneur, C.: A synthesis of progress and uncertainties in
355 attributing the sources of mercury in deposition, *Ambio*, 36, 19-32, 2007.
- 356
357 Meehl, G.A.: The South Asian monsoon and the tropospheric biennial oscillation, *J.*
358 *Climate*, 10, 1921-1943, 1997.
- 359
360 Meehl, G.A., and Arblaster, J.M.: The tropospheric biennial oscillation and Indian
361 monsoon rainfall, *Geophys. Res. Lett.*, 28, 1731-1734, 2001.
- 362
363 Meehl, G.A., and Arblaster, J.M.: The tropospheric biennial oscillation and Asian-
364 Australian monsoon rainfall, *J. Climate*, 15, 722-744, 2002.
- 365
366 Mergler, D., Anderson, H.A., Chan, L.H.N., Mahaffey, K.R., Murray, M., Sakamoto,
367 M., and Stern, A.H.: Methylmercury exposure and health effects in humans: A
368 worldwide concern, *Ambio*, 36, 3-11, 2007.
- 369
370 Muntean, M., Janssens-Maenhout, G., Song, S., Selin, N.E., Olivier, J.G.J., Guizzardi,
371 D., Maas, R., Dentener, F.: Trend analysis from 1970 to 2008 and model evaluation of

- 372 EDGARv4 global gridded anthropogenic mercury emissions, *Sci. Total Environ.* 494-
373 495, 337-350, 2014.
- 374
- 375 Pacyna, J.M., Travnikov, O., De Simone, F., Hedgecock, I.M., Sundseth, K., Pacyna,
376 E.G., Steenhuisen, F., Pirrone, N., Munthe, J., and Kindbom, K.: Current and future
377 levels of mercury atmospheric pollution on a global scale, *Atmos. Chem. Phys.*, 16,
378 12495-12511, 2016.
- 379
- 380 Prestbo, E.M., and Gay, D.A.: Wet deposition of mercury in the U.S. and Canada, 1996-
381 2005: Results and analysis of the NADP mercury deposition network (MDN), *Atmos.*
382 *Environ.* 43, 4223-4233, 2009.
- 383
- 384 Rotty, R.M.: Estimates of seasonal variation in fossil fuel CO₂ emission, *Tellus B*, 39,
385 184–202, 1987.
- 386
- 387 Salmi, T., Määttä, A., Anttila, P., Ruoho-Airola, T., Amnell, T.: Detecting trends of
388 annual values of atmospheric pollutants by the Mann-Kendall test and Sen's slope
389 estimates – the Excel template application Makesens, Finnish Meteorological Institute,
390 Helsinki, Finland, 2002.
- 391
- 392 Scheuhammer, A.M., Meyer, M.W., Sandheinrich, M.B., and Murray, M.W.: Effects
393 of environmental methylmercury on the health of wild birds, mammals, and fish,
394 *Ambio*, 36, 12-18, 2007.
- 395
- 396 Selin, N.E., Jacob, D.J., Yantoska, R.M., Strode, S., Jaeglé, L., and Sunderland, E.M.:
397 Global 3-D land-ocean-atmosphere model for mercury: Present-day versus
398 preindustrial cycles and anthropogenic enrichment factors for deposition, *Global*
399 *Biogeochem. Cycles*, 22, GB2011, doi:10.1029/2007GB003040, 2008.
- 400
- 401 Selin, N. E.: Global biogeochemical cycling of mercury: A review, *Ann. Rev. Environ.*
402 *Resour.*, 34, 43–63, doi:10.1146/annurev.environ.051308.084314, 2009.
- 403
- 404 Slemr, F., Brunke, E.-G., Labuschagne, C., Ebinghaus, R.: Total gaseous mercury
405 concentrations at the Cape Point GAW station and their seasonality, *Geophys. Res. Lett.*
406 35, L11807, doi:10.1029/2008GL033741, 2008.
- 407
- 408 Slemr, F., Brunke, E.-G., Ebinghaus, R., Kuss, J.: Worldwide trend of atmospheric
409 mercury since 1995, *Atmos. Chem. Phys.* 11, 4779-4787, 2011.
- 410
- 411 Slemr, F., Brenninkmeijer, C.A.M., Rauthe-Schöch, A., Weigelt, A., Ebinghaus, R.,
412 Brunke, E.-G., Martin, L., Spain, T.G., and O'Doherty, S.: El Niño – Southern
413 Oscillation influence on tropospheric mercury concentrations, *Geophys. Res. Lett.*, 43,
414 1766-1771, 2016.
- 415
- 416 Soerensen, A.L., Jacob, D.J., Streets, D.G., Witt, M.L.I., Ebinghaus, R., Mason, R.P.,
417 Andersson, M., Sunderland, E.M.: Multi-decadal decline of mercury in the North-
418 Atlantic atmosphere explained by changing subsurface seawater concentrations,
419 *Geophys. Res. Lett.* 39, L21810, doi:10.1029/2012GL053736, 2012.
- 420

- 421 Sprovieri, F., Pirrone, N., Ebinghaus, R., Kock, H., and Dommergue, A.: A review of
422 worldwide atmospheric mercury measurements, *Atmos. Chem. Phys.*, 10, 8245-8265,
423 2010.
- 424
- 425 Sprovieri, F., Pirrone, N., Bencardino, M., D'Amore, F., Carbone, F., Cinnirella, S.,
426 Mannarino, V., Landis, M., Ebinghaus, R., Weigelt, A., Brunke, E.-G., Labuschagne,
427 C., Martin, L., Munthe, J., Wängberg, I., Artaxo, P., Morais, F., Cairns, W., Barbante,
428 C., del Carmen Diéguez, M., Garcia, P.E., Dommergue, A., Angot, H., Magand, O.,
429 Skov, H., Horvat, M., Kotnik, J., Read, K.A., Neves, L.M., Gawlik, B.M., Sena, F.,
430 Mashyanov, M., Obolkin, V.A., Wip. D., Feng, X.B., Zhang, H., Fu, X.,
431 Ramachandran, R., Cossa, D., Knoery, J., Maruszczak, N., Nerentorp, N., and
432 Norstrom, C.: Atmospheric mercury concentrations observed at ground-based
433 monitoring sites globally distributed in the framework of the GMOS network, *Atmos.*
434 *Chem. Phys. Discuss.*, doi:10.5194/acp-2016-466, 2016.
- 435
- 436 Streets, D.G.; Devane, M.K., Lu, Z., Bond, T.C., Sunderland, E.M., and Jacob, D.J.:
437 All-time releases of mercury to the atmosphere from human activities, *Environ. Sci.*
438 *Technol.*, 45, 10485-10491, 2011.
- 439
- 440 Temme, C., Planchard, P., Steffen, A., Banic, C., Beauchamp, S., Poissant, L., Tordon,
441 R., and Wiens, B.: Trend, seasonal and multivariate analysis study of total gaseous
442 mercury data from the Canadian Atmospheric Mercury Measurement Network (CAM-
443 Net), *Atmos. Environ.*, 41, 5423-5441, 2007.
- 444
- 445 Tohir, A.M., Venkataraman, S., Mbatha, N., Sangeetha, S.K., Bencherif, H., Brunke,
446 E.-G. and Labuschagne, C. (2015). Studies on CO variation and trends over South
447 Africa AUTHORS: and the Indian ocean using TES satellite data. *South African*
448 *Journal of Science*; <http://www.sajs.co.za> Volume 111; Number 9/10 Sep/Oct 2015.
- 449
- 450 Van der Werff, G.R., Randerson, J.T., Giglio, L., Collatz, G.J., Kasibhatla, T.S., and
451 Arellano, Jr., A.F.: Interannual variability in global biomass burning emissions from
452 1997 to 2004, *Atmos. Chem. Phys.*, 6, 3423-3441, 2006.
- 453
- 454 Weigelt, A., Ebinghaus, R., Manning, A.J., Derwent, R.G., Simmonds, P.G., Spain,
455 T.G., Jennings, S.G., Slemr, F.: Analysis and interpretation of 18 years of mercury
456 observations since 1996 at Mace Head at the Atlantic Ocean coast of Ireland, *Atmos.*
457 *Environ.* 100, 85-93, 2015.
- 458
- 459 Weiss-Penzias, P.S., Gay, D.A., Brigham, M.E., Parsons, M.T., Gustin, M.S., and ter
460 Schure, A.: Trends in mercury wet deposition and mercury air concentrations across the
461 U.S. and Canada, *Sci. Total Environ.*, 568, 546-556, 2016.
- 462
- 463 Wilson, S., Munthe, J., Sundseth, K., Kindbom, K., Maxson, P., Pacyna, J., and
464 Steenhuisen, F.: Updating historical global inventories of anthropogenic mercury
465 emissions to air, AMAP Technical Report No. 3, 14 pp, *Arct. Monit. And Assess.*
466 *Programme*, Oslo, 2010.
- 467
- 468 Zhang, Y., Jacob, D.J., Horowitz, H.M., Chen, L., Amos, H.M., Krabbenhoft, D.P.,
469 Slemr, F., Louis, V.L.St., and Sunderland, E.M.: Observed decrease in atmospheric

470 mercury explained by global decline in anthropogenic emissions, PNAS, 113, 526-531,
471 2016.
472
473 Zheng, B., and Liang, J.-Y.: Advance in studies of tropospheric biennial oscillation, J.
474 Tropical Meteorol., 11, 1-9, 2005.
475

476 **Tables**

477

478 Table 1: Sen's slopes calculated from monthly GEM averages of all and baseline (i.e. $^{222}\text{Rn} \leq$
 479 250 mBq m^{-3}) data for March 2007 – June 2015.

Data	Sen's slope [$\text{ng m}^{-3} \text{ year}^{-1}$]	n	Significance [%]	Range at 95% signif. level [$\text{ng m}^{-3} \text{ year}^{-1}$]
All data	0.0210	99	>99.98	0.0127 – 0.0284
All Baseline	0.0208	97	>99.98	0.0141 – 0.0280
Fall (MAM, all data)	0.0089	27	95.99	-0.0009 – 0.0198
Fall (MAM, baseline)	0.0108	27	98.78	0.0018 – 0.0223
Winter (JJA, all data)	0.0153	25	99.29	0.0025 – 0.0294
Winter (JJA, baseline)	0.0152	25	98.68	0.0020 – 0.0287
Spring (SON, all data)	0.0375	24	99.74	0.0142 – 0.0556
Spring (SON, baseline)	0.0361	24	99.84	0.0160 – 0.0563
Summer (DJF, all data)	0.0287	23	99.87	0.0119 – 0.0440
Summer (DJF, baseline)	0.0269	21	99.79	0.0020 – 0.0287

480

481

482 Table 2: Least square fit of monthly median of all GEM concentrations for September
 483 1995 – December 2004.

484

Data	Slope [$\text{ng m}^{-3} \text{ year}^{-1}$]	n	Signif. level [%]
All data	-0.0176 ± 0.0027	94	>99.9
Fall (MAM)	-0.0132 ± 0.0052	23	>95
Winter (JJA)	-0.0189 ± 0.0049	23	>99.9
Spring (SON)	-0.0198 ± 0.0038	24	>99.9
Summer (DJF)	-0.0154 ± 0.0065	24	>95

485

486

487

488

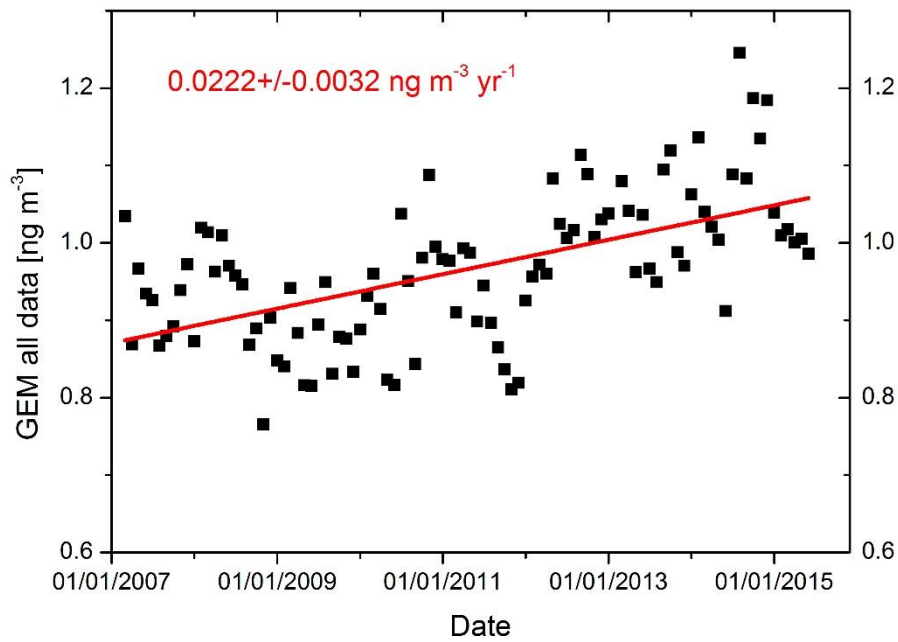
489

490

491

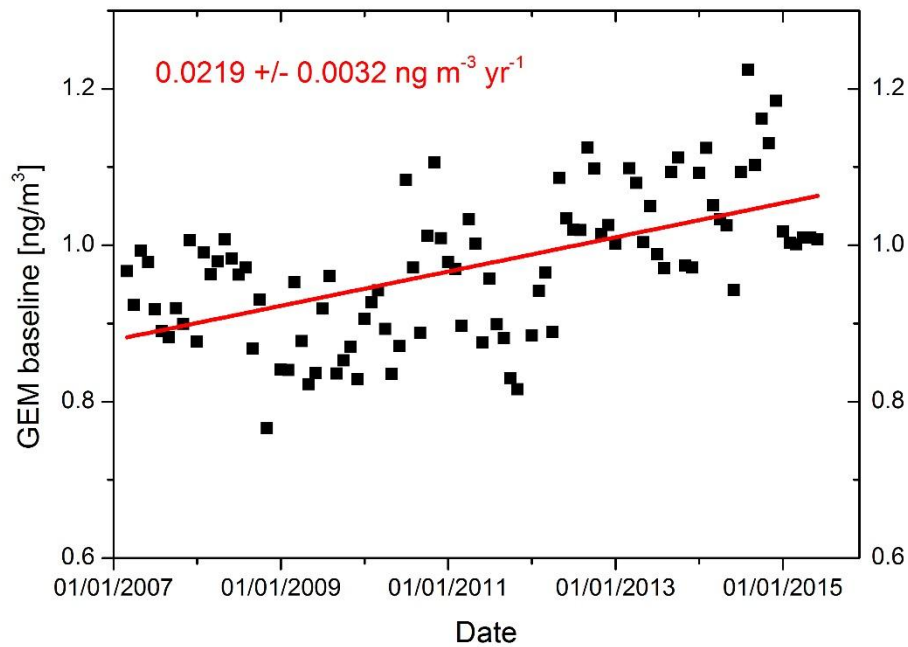
492 **Figures**

493



494

495



496

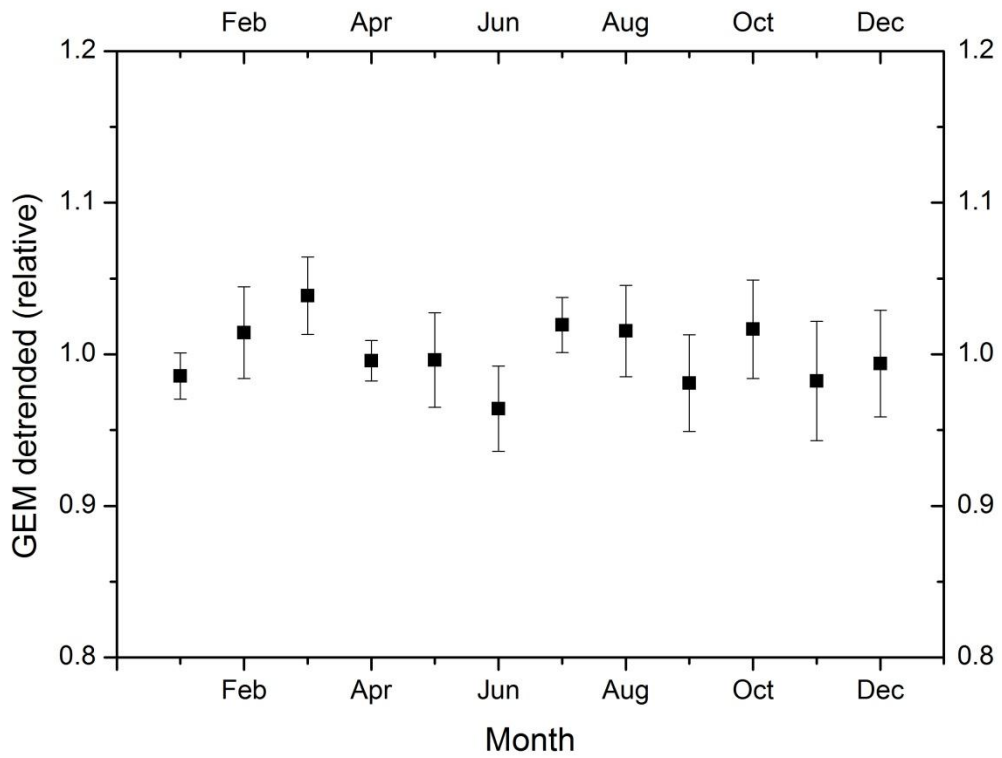
497

498 Figure 1: Monthly average GEM concentrations and their least square fit: upper panel

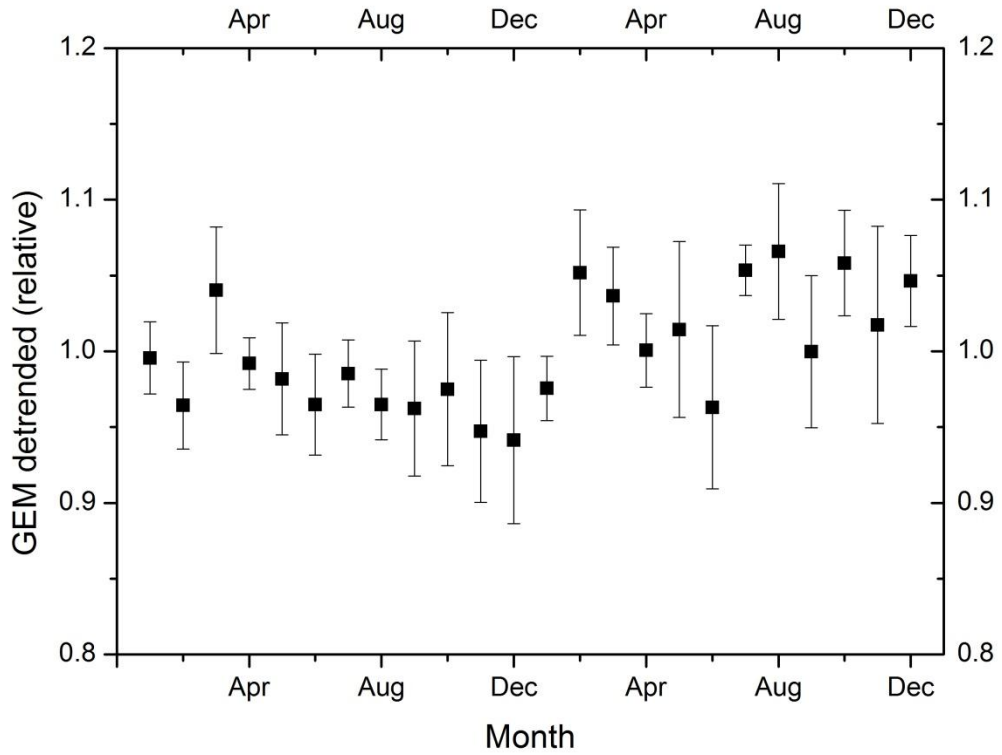
499 all data, lower panel baseline data (i.e. only GEM concentrations at ^{222}Rn 500 concentrations $\leq 250 \text{ mBq m}^{-3}$.

501

502



503
504



505
506

507 Figure 2: Seasonal (upper panel) and biennial (lower panel) variation of detrended
508 monthly averages. The error bars denote the standard error of the monthly average.

